

REPORT DOCUMENTATION PAGE

Form Approved
OMB No. 0704-0188

Public reporting burden for this collection of information is estimated to average 1 hour per response, including the time for reviewing instructions, searching existing data sources, gathering and maintaining the data needed, and completing and reviewing this collection of information. Send comments regarding this burden estimate or any other aspect of this collection of information, including suggestions for reducing this burden to Department of Defense, Washington Headquarters Services, Directorate for Information Operations and Reports (0704-0188), 1215 Jefferson Davis Highway, Suite 1204, Arlington, VA 22202-4302. Respondents should be aware that notwithstanding any other provision of law, no person shall be subject to any penalty for failing to comply with a collection of information if it does not display a currently valid OMB control number. PLEASE DO NOT RETURN YOUR FORM TO THE ABOVE ADDRESS.

1. REPORT DATE (DD-MM-YYYY)		2. REPORT TYPE Technical Papers		3. DATES COVERED (From - To)	
4. TITLE AND SUBTITLE				5a. CONTRACT NUMBER	
				5b. GRANT NUMBER	
				5c. PROGRAM ELEMENT NUMBER	
6. AUTHOR(S)				5d. PROJECT NUMBER	
				5e. TASK NUMBER	
				5f. WORK UNIT NUMBER	
7. PERFORMING ORGANIZATION NAME(S) AND ADDRESS(ES) Air Force Research Laboratory (AFMC) AFRL/PRS 5 Pollux Drive Edwards AFB CA 93524-7048				8. PERFORMING ORGANIZATION REPORT	
9. SPONSORING / MONITORING AGENCY NAME(S) AND ADDRESS(ES) Air Force Research Laboratory (AFMC) AFRL/PRS 5 Pollux Drive Edwards AFB CA 93524-7048				10. SPONSOR/MONITOR'S ACRONYM(S)	
				11. SPONSOR/MONITOR'S NUMBER(S)	

12. DISTRIBUTION / AVAILABILITY STATEMENT Approved for public release; distribution unlimited.		20020823 064	
-------------------------------------------------------------------------------------------------------	--	--------------	--

6340 RH6S

TP-FY99-0126

✓ Spreadsheet
✓ DTB

MEMORANDUM FOR PRR (Contractor/In-House Publication)

FROM: PROI (TI) (STINFO)

2 June 1999

SUBJECT: Authorization for Release of Technical Information, Control Number: AFRL-PR-ED-TP-FY99-0126
Fife, LeDuc, Sutton and Bromaghim, AIAA-99-2707, "Preliminary Orbital Performance Analysis of the Air Force Electric Propulsion Space Experiment (ESEX) Ammonia Arcjet"
AIAA Joint Propulsion Conference (Public Release)

15. SUBJECT TERMS				
16. SECURITY CLASSIFICATION OF:		17. LIMITATION OF ABSTRACT	18. NUMBER OF PAGES	19a. NAME OF RESPONSIBLE PERSON
a. REPORT	b. ABSTRACT	A		Leilani Richardson
Unclassified	Unclassified			19b. TELEPHONE NUMBER (include area code)
c. THIS PAGE	Unclassified			(661) 275-5015

41 items enclosed

FLIGHT MEASUREMENTS

Accelerometer

The onboard Servo Accelerometer Assembly (SAA) measures spacecraft acceleration continually at 10 Hz. The SAA housing is 2.2 x 2.8 x 5.5 inches and contains an Allied Signal QA-3000-001 servo accelerometer and associated amplifier, bias, and filter electronics. The QA-3000-001 is the closed-loop servo type with a fused quartz proof mass pendulum. The signal from the SAA is digitized and recorded by the ESEX CCU. This digital data is then polled by ARGOS and recorded for downlink to a ground station. Figure 1 shows the signal/data path.

The 2500-kg spacecraft accelerates at approximately 80 μg due to the 2-N arcjet thrust. To measure this small acceleration, the Allied Signal QA-3000-010 accelerometer was chosen, the performance properties of which are given in Table 1.

Measurement Range	+/- 25 μg
Resolution	1 μg
Unbiased Output Noise at DC to 10 Hz	10 μg

Table 1. QA-3000-001 accelerometer performance.

Although the resolution of the accelerometer is 1 μg , the amplifier electronics and A/D converter are designed to give a lower resolution of 2.44 μg . This is because the SAA electronics amplify and bias the signal from the accelerometer to the range 0 to 10V corresponding to -5 to 5 mg. With this wide acceleration range, one bit of the 12-bit 0-to-10V A/D converter corresponds to 2.44 μg .

Therefore, using the SAA, accelerations can only be determined to within 2.44 μg , or about 3% of nominal acceleration during arcjet firing. This is a "best case." In fact, the uncertainty in the acceleration estimate will be shown to be around 4.7% due to other factors.

The accelerometer output current is proportional to input acceleration. This current is passed through a 20 k Ω resistor. The voltage across the resistor is then filtered, amplified, and biased by the electronics in the SAA. The resulting signal output from the SAA (0 to 10V) is digitized in the CCU and made available for downlink.

A complete end-to-end (acceleration to digital number) calibration of the accelerometer system was not done. Therefore, individual calibration parameters for each component must be determined and combined. Additional complications in the calibration arise because the original flight accelerometer unit failed during vibration tests⁹. It was replaced with a second unit, but all tests and calibrations were not repeated for the second unit.

Allied Signal documentation¹⁰ for the QA-3000-001 gives formulas for determining input acceleration from output current,

$$a = \frac{I}{SF(T)} - BIAS(T), \quad (1)$$

where a is the input acceleration, I is the output current, $SF(T)$ is the scale factor, and T is the accelerometer temperature. $SF(T)$ and $BIAS(T)$ are determined at Allied Signal, and their values are listed in the acceptance test data.¹¹ They are given as fourth-order polynomial functions of accelerometer temperature. An on-board sensor (also calibrated at Allied Signal) measures accelerometer temperature. The signal is amplified and biased by a separate set of electronics in the SAA, the output of which is digitized at the CCU and made available to ARGOS for downlink.

The SAA electronics amplify and bias the accelerometer signal. A model for this process is,

$$V_a = F_0 + F_1 IR, \quad (2)$$

where V_a is the SAA accelerometer output voltage, R is the SAA input resistance, and F_0 and F_1 are calibration parameters. During ground calibration¹², temperature dependence of F_0 and F_1 was found to cause less than 0.078 percent error in the nominal (80 μg) reading per degrees Fahrenheit. This is much smaller than the temperature dependence of the accelerometer and is ignored. The coefficients F_0 and F_1 are determined by a linear fit of Equation 2 using data from the Final Functional Test.¹² The calibration coefficients (using the later data) are given below.

F_0	3.723 V
F_1	38.91
R	20 k Ω

The A/D converter was not calibrated on the ground. Therefore, the A/D converter is assumed to be an ideal 0-10V 12-bit linear device with integer output, x , equal to $2^{12}V_a/10$.

Measurements during ESEX flight at 0g indicate a shift in the accelerometer bias 225 μg lower than measured on the ground.¹² This bias is within specification for the device. However, Equation 1 must be changed to reflect the drift. A new model for the accelerometer is,

$$a = \frac{I}{SF(T)} - BIAS(T) - BIAS2, \quad (3)$$

where $BIAS2(T)$ is determined from the zero-g point 30 seconds before initiation of each respective firing. Combining Equation 3 with Equation 2,

$$a = \frac{V_a - F_0}{F_1 R SF(T)} - BIAS(T) - BIAS2. \quad (4)$$

Above, $V_a = 10x/2^{12}$ from the "calibration" of the A/D converter.

To calculate the mean acceleration for a given firing, the arithmetic mean of each parameter is used in Equation 4 for the period 30 seconds before shut-off of the arcjet discharge:

$$\bar{a} = \frac{\bar{V}_a - F_0}{F_1 R \bar{SF}(T)} - \bar{BIAS}(T) - BIAS2. \quad (5)$$

Table title above, not beneath table

This method is used (versus using the mean of the accelerations calculated instantaneously at each point) because of its simplicity. It is believed to be valid because no correlation between measurements is seen. Furthermore, any correlation that does exist will only result as second-order error.

The uncertainty in the estimate of mean acceleration, $u(\bar{a})$, can be derived using the combined uncertainty laws.¹³ It can be shown that the dependence on T is negligible in the calculation of uncertainty, so,

$$\bar{a} = \frac{\bar{V}_a - F_0}{F_1 R S F} - \overline{BIAS} - BIAS2. \quad (6)$$

It is important to note that \bar{a} is not actually calculated with constant T . We use this approximation only in our estimate of uncertainty. Subtracting from the zero-g state (indicated by the 0-subscript),

$$\bar{a} = \frac{\bar{V}_a - \bar{V}_{a,0}}{F_1 R S F}. \quad (7)$$

The combined uncertainty for this expression is,

$$u(\bar{a}) = \bar{a} \left[\frac{u^2(\bar{V}_a) + u^2(\bar{V}_{a,0})}{(\bar{V}_a - \bar{V}_{a,0})^2} + \frac{u(F_1)^2}{F_1^2} + \frac{u(R)^2}{R^2} + \frac{u(SF)^2}{SF^2} \right]^{1/2}. \quad (8)$$

The uncertainty in V_a is a root sum of squares of the experimental standard deviation, $\sigma_{\bar{V}_a}$, and the uncertainty due to the discretization of the A/D converter, $u(A/D)$. The A/D converter uncertainty, $u(A/D)$, is assumed to be 2.44×10^{-3} V, which corresponds to one bit of resolution. Based on $n=30$ samples of V_a at 1 Hz, and for $\sigma_{\bar{V}_a} = 0.00253$ V (Firing 5), we find $u(V_a) = 0.00248$ V. The uncertainty in F_1 is found to be 0.214 . The uncertainty in R is 0.1% from TRW schematics. The uncertainty in SF is 2.05×10^{-5} mA/g, corresponding to the 15.83 ppm residual in the Allied Signal calibration. Finally, using Equation 8 for Firing 5, we have $u(\bar{a}) = 3.44 \mu\text{g}$, or 4.44% of nominal. Table 3 shows a summary of the relative contributions of each uncertainty component for each firing.

Using the calibration described above, the accelerometer voltage signals for each firing are converted to acceleration signals by application of Equation 4 at each data point. The voltage and acceleration for Firing 5 are given in Figures 2 and 3, respectively. The initial $8\text{-}\mu\text{g}$ acceleration is due to initial propellant release prior to initiation of the electrical discharge. In this mode, the arcjet is operating as a cold-gas thruster with ammonia propellant. The ramp in acceleration from 8 to $76 \mu\text{g}$ is due to a programmed start-up sequence in the PCU. After the ramp, the PCU switches to constant power mode at approximately 26 kW. The exponential drop-off of acceleration occurs after the arcjet discharge is shut off. Nominal flow continues for two minutes after shut-off, generating additional thrust that drops off as the arcjet cools.

Propellant Flow Rate

The propellant flow system (PFS) on ESEX uses a sonic venturi to measure ammonia flow rate. There are three principal sources of error in this method. They are the calibration error of the sonic venturi, the error of the pressure transducer, and the error of the thermocouple. A review of the sonic venturi calibration data indicates an uncertainty of 2.2% at 240 mg/sec. The pressure transducer was qualified and

acceptance tested to a requirement of 1.0% of full-scale, which was 250 psia. These yield an error of 3.9% at the steady-state operating pressures observed. Calibration data for the thermocouple is no longer available. However, typical thermocouple measurement variation would be about ± 5 deg F in this measurement range, which yields an error of only about 1.0% of the absolute measured temperature used in the flow calculation. A root sum of squares combination of these errors is approximately 4.5%. The confidence limit for these errors is 95%. These errors appear to be significantly larger than the encoding error resulting from the 32-bit data word.

PCU

The PCU controls discharge current level by controlling the duty cycle of FET hybrid switches. There are three parallel phases of power converters within the PCU 120 degrees out of phase with each other. Within each phase block, there are a pair of current sense transformers that effectively measure the total current out from each of the phases, each switching cycle. The output of the six current sense transformers is electronically summed together and integrated for each cycle, and that signal is compared with the current reference voltage that indicates the desired current level for the PCU. The output of this comparison affects the duty cycle of the converter hybrid switches, which in turn ~~are what~~ governs the actual DC output current level.

During on-orbit thruster firings, the voltage and current telemetry consistently indicated a power reading of 27.9 ± 0.05 kW, relative to the specified 26.0 ± 0.78 kW. An examination of the data, both on orbit and during ATP at PAC in 1994, indicate strongly that the power reading is higher than actual, due, most likely, to a drift in the telemetry current shunt. Arcjet temperatures and on-orbit performance data corroborate this conclusion. Furthermore, the design of the PCU is resistant to changes in power. Therefore, the voltage and current telemetry ~~is~~ considered erroneous and thrown out. The PCU is treated as a constant-power device, with actual power levels corresponding to those during acceptance tests, $26.2 \text{ kW} \pm 1.5\%$.

GPS

It was the intent of the ESEX team to use the Global Positioning System (GPS) receiver on board ARGOS to make an assessment of the ESEX arcjet performance independent of the EXEX accelerometer.

The GPS receiver, required by the ARGOS program office, delivers position, velocity, and Coordinated Universal Time (UTC) at 1 Hz. The receiver is able to acquire and track five channels of the L1 (1575.42 MHz) C/A-code. The accuracy of the receiver without selective availability enabled is 15 m of position error, 0.1 m/s RMS per axis velocity error, and 300 ns (1 sigma) time error. The requirements with selective availability turned on were 76-100 m position error, 0.5 m/s RMS per axis velocity error, and 1 μs (1 sigma) time error.

Due to problems with the GPS receiver dropping out of navigation mode into acquisition mode, GPS data was only collected for Firing 1. Furthermore, latency problems integral to the design of the receiver complicate the analysis of the resulting data. Nevertheless, this data is currently under

analysis by The Aerospace Corporation. Preliminary results substantiate accelerometer performance measurements for Firing 1, but a detailed description of the analysis must be published at a later date.

Radar Ranging

Radar ranging from the Air Force Satellite Control Network (AFSCN) was also used as an independent measurement of ΔV produced by arcjet firings. Multiple tracking data points were used to determine ~~reduced to determine~~ the change in semi-major axis during each thruster firing. Then, using orbital motion equations, and assuming axial retrograde thrust, estimates of ΔV were calculated. Determination of the uncertainty in these estimates is in progress.

ADACS

The ARGOS Attitude Determination and Control System (ADACS) consists of two Inertial Reference Units (IRU), two Scanning Horizon Sensors (SHS), six Sun Sensors Analog (SSA), four Reaction Wheels (RW), two Electromagnets (EM), one magnetometer, and related software.¹⁵ For the purposes of determining the off-axis thrust from ESEX arcjet firings, the behavior of the reaction wheels is of primary interest. An analysis of ARGOS reaction wheel data and determination of the off-axis thrust from the ESEX arcjet will be presented in a later publication.

Mass History

The spacecraft mass is estimated to be 2487.19 kg. This is derived from pre-launch measurements and a tally of mass release events. It is believed to be within ^{0.2}2% of the actual value.

ANALYSIS AND DISCUSSION

Although accelerometer voltages were recorded at 10 Hz (¹⁰telemetry record), Figures 2 and 3 show data at only 1 Hz. All other performance data (flow rate and discharge power) were recorded at 1 Hz. Therefore, for purposes of evaluating thruster performance, only the 1 Hz data (taken simultaneous with flow rate and discharge power) is considered.

To ensure that performance data reflects conditions at the steady-state nominal operating condition, only the last 30 seconds of each firing are used. Average acceleration is determined from the individual averages of the accelerometer voltage, scaling factor, and bias over that 30-second period. Likewise, performance parameters are determined from the individual 30-second averages of the acceleration, flow rate, and discharge power. Only firings 1 through 6 reached full power, so those are the only firings for which performance data is presented.

Table 4 shows a summary of the performance findings using the calibrated accelerometer data. The uncertainty numbers are based on analysis presented in the earlier sections.

Figure 4 plots the specific impulse results from each firing in comparison with ground data. The lines represent the bounds

on the original performance specification for the arcjet. The vertical error bars represent uncertainty in I_{sp} , and are calculated by the procedure discussed earlier, but also taking into account the uncertainty in flow rate. The horizontal error bars represent the combined standard uncertainty for P/\dot{m} .

A final performance figure for the flow rate 250 mg/s can be determined as the mean of the five 30-second means. A standard combined uncertainty estimate is used,

$$\begin{aligned} \bar{I}_{sp} &= \frac{1}{\sqrt{5}} \left[u(\bar{I}_{sp,1})^2 + u(\bar{I}_{sp,2})^2 + \dots + u(\bar{I}_{sp,5})^2 \right]^{1/2}, \\ u(\bar{\eta}) &= \frac{1}{\sqrt{5}} \left[u(\bar{\eta}_1)^2 + u(\bar{\eta}_2)^2 + \dots + u(\bar{\eta}_5)^2 \right]^{1/2}. \end{aligned} \quad (9)$$

This gives, for the 250 mg/s flow rate,

$$\begin{aligned} \bar{I}_{sp} &= 787.0 \pm 49.8 \text{ seconds} \\ \bar{\eta} &= 0.284 \pm 0.029 \end{aligned}$$

The original design specification for the arcjet¹⁶ lists I_{sp} and η as 800 seconds and 30.7%, respectively. However, the best thruster performance achieved with the engineering model on the ground was 799 seconds at 27.2% efficiency.¹⁷

It is believed that deviation in the thrust vector will affect the performance numbers, but not in a significant way because the measured acceleration is a weak function (cosine) of the angle between the thrust vector and the accelerometer axis. Quantification of the off-axis thrust is saved for the future when ADACS data can be analyzed.

Total velocity change is obtained from accelerometer data by integration of the acceleration curve. The trapezoidal rule was used, and the uncertainty was computed based strictly on systematic sources (A/D converter resolution, F_i , R , and SF) assuming the random components cancel. Those numbers are shown in Table 5 in comparison to results from radar ranging and GPS.

Figure 5 shows a graphical comparison between ΔV from accelerometer data and ΔV from radar ranging. The line represents a linear least squares fit. If the accelerometer measurements differ from the ranging data by a scaling factor, that factor should be proportional to the line of fit. The slope of the fit is 0.9864, indicating only 1.36% scaling factor error, with a RMS relative residual of 2.07%. Thus, the accelerometer data correlate very well with the radar ranging data for all 6 firings. Firing 3 clearly has the greatest error. If that data point is disregarded (as likely due to a mistake in ranging), the agreement improves, with error less than 1%. This suggests that the uncertainty of the accelerometer-derived performance estimates of 7 to 10% percent may be too conservative. Furthermore, the apparent changes in performance between firings appear to be validated by the ranging data.

SUMMARY

Based on accelerometer data alone, mean arcjet specific impulse on orbit is 1.6% below design specification. Thrust efficiency is 7.5% below design specification. However, compared to ground tests, on-orbit specific impulse is 1.5% low, and efficiency is 4.4% high. Although estimates of

COL-
↑
SENTENCE

I THOUGHT
↑
FIRING 1 WAS

uncertainty in measured acceleration are large (4.44%), measurements from GPS and radar ranging independently support the accuracy of the accelerometer data.

REFERENCES

¹Kriebel, M. M. and Stevens, N. J., "30-kW Class Arcjet Advanced Technology Transition Demonstration (ATTD) Flight Experiment Diagnostic Package," AIAA Paper 92-3561, July 1992.

²Sutton, A. M., Bromaghim, D. R., and Johnson, L. K., "Electric Propulsion Space Experiment (ESEX) Flight Qualification and Operations," AIAA Paper 95-2503, July 1995. Also presented as a JANNAF Paper, December 1995.

³LeDuc, J. R., et. al., "Performance, Contamination, Electromagnetic, and Optical Flight Measurement Development for the Electric Propulsion Space Experiment," AIAA Paper 96-2727, July 1996.

⁴Turner, B. J. and Agardy, F. J., "The Advanced Research and Global Observation Satellite (ARGOS) Program," AIAA Paper 94-4580, September 1994.

⁵Agardy, F. J. and Cleave, R. R., "A Strategy for Maximizing the Scientific Return Using a Multi-phased Mission Design for ARGOS," AAS 93-594, August 1993.

⁶Vaughan, C. E., and Morris, J. P., "Propellant Feed Subsystem for a 26 kW Flight Arcjet Propulsion System," AIAA-93-2400, June 1993.

⁷Biess, J. J. and Sutton A. M., "Integration and Verification of a 30 kW Arcjet Spacecraft System," AIAA Paper 94-3143, June 1994.

⁸Vaughan, C. E., Cassady, R. J., and Fisher, J. R., "Design, Fabrication, and Test of a 26 kW Arcjet and Power Conditioning Unit," IEPC-93-048, September, 1993.

⁹TRW Test Discrepancy Report TL6468, March, 1995.

¹⁰Product Specification for 979-3000-001 Accelerometer, Allied Signal, February 1998.

¹¹Acceptance Test Data, Allied Signal P/N 979-3000-001 T/A S/N 331, February 1995.

¹²Arcjet ATTD Functional Test Procedure for Servo Accelerometer Assembly (SAA) and associated data sheets, TRW, April 1996.

¹³American National Standard for Expressing Uncertainty - U.S. Guide to the Expression of Uncertainty in Measurement, ANSI/NCSL Z540-2-1997, October 1997.

¹⁴Boeing North American, Inc., "Integrated Electronics Unit Specification", Boeing Control Number KC091-0001-0001, 8 November 1997.

¹⁵Boeing North American, Inc., "P91-1 Orbital Operations Handbook, Revision C", USAF Contract No. F04701-91-C-0090, CDRL A006, 15 April 1999.

¹⁶Primex Aerospace Corp., 30kWe Class Arcjet Design Specification, July 1991.

¹⁷Olin Aerospace Corp., Arcjet Advanced Technology Demonstration (ATTD) Engineering Model Test Report, April 11, 1995.

ck out

ck out
ck out

ck out

ck out

ck out

ck out

W42RE
15 RET#14
REC'D FROM 70

Firing	Date	Time (Zulu)	Duration	Flow Rate (mg/s)	Remarks
1	03/15/99	21:55:56	2:20	240	
2	03/19/99	22:32:24	5:02	250	
3	03/21/99	12:24:42	5:34	250	
4	03/23/99	21:27:59	8:02	250	
5	03/26/99	12:45:29	6:05	250	
6	03/31/99	13:05:36	4:31	250	Shut-off due to low battery voltage
7a	04/02/99	22:09:03	0:55	250	Shut-off due to low battery voltage
7b	04/02/99	22:10:08	0:37	250	Shut-off due to low battery voltage
8	04/21/99	12:22:13	0:43	250	Shut-off due to low battery voltage

Table 2. Arcjet firing summary.

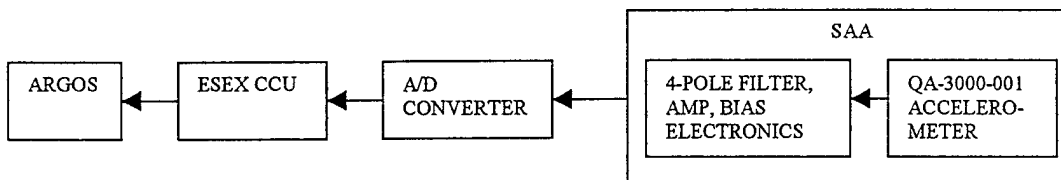


Figure 1. Accelerometer signal/data path.

Accelerometer output voltage A/D converter uncertainty	$\frac{\sqrt{2}u(A/D)}{(\bar{V}_a - \bar{V}_{a,0})}$	4.52E-02	4.38E-02	4.18E-02	4.45E-02	4.36E-02	4.27E-02
Accelerometer output voltage experimental standard deviation	$\sqrt{\frac{\sigma_{\bar{V}_a}^2 + \sigma_{\bar{V}_{a,0}}^2}{(\bar{V}_a - \bar{V}_{a,0})^2}}$	1.26E-02	9.31E-03	6.60E-03	1.40E-02	5.84E-03	2.32E-03
Amplifier calibration parameter uncertainty	$\frac{u(F_1)}{F_1}$	5.49E-03	5.49E-03	5.49E-03	5.49E-03	5.49E-03	5.49E-03
Input resistance uncertainty	$\frac{u(R)}{R}$	1.00E-03	1.00E-03	1.00E-03	1.00E-03	1.00E-03	1.00E-03
Accelerometer scaling factor uncertainty	$\frac{u(\overline{SF})}{\overline{SF}}$	1.58E-05	1.58E-05	1.58E-05	1.58E-05	1.58E-05	1.58E-05

Table 3. Relative contributions to uncertainty of mean acceleration.

SHOULD
COLUMNS

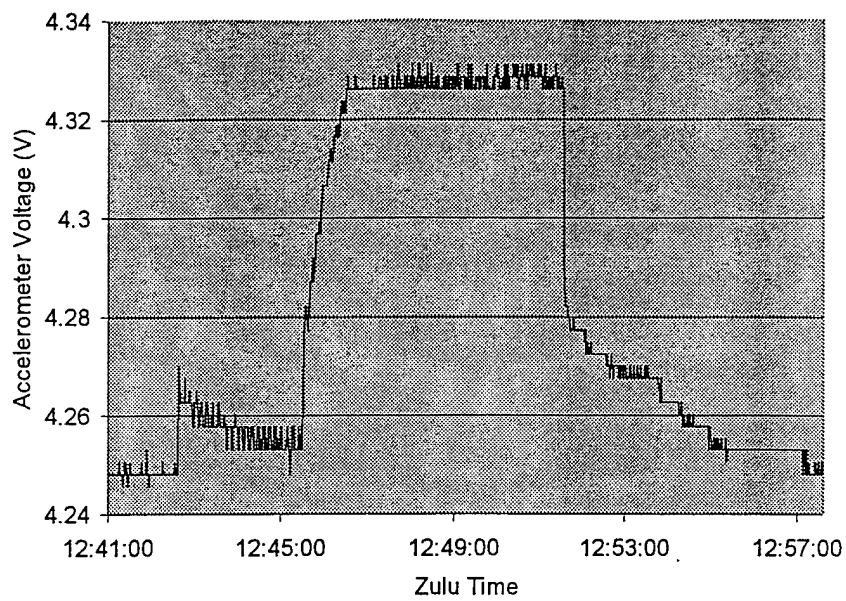


Figure 2. Accelerometer voltage during Firing 5.

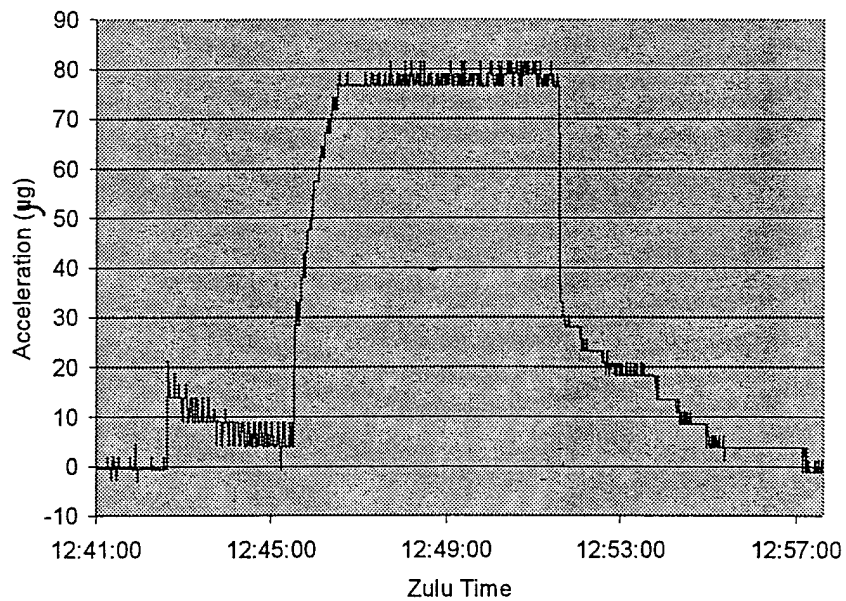


Figure 3. Calibrated acceleration during Firing 5.

Firing	Mean Acceleration, \bar{a} (μg)	Mean Thrust, F (N)	Mean Specific Impulse, I_{sp} (s)	Mean Efficiency, η
1	76.07 \pm 3.60	1.855 \pm 0.088	789.0 \pm 51.5	0.274 \pm 0.029
2	78.98 \pm 3.57	1.926 \pm 0.087	786.1 \pm 50.1	0.284 \pm 0.029
3	80.97 \pm 3.46	1.975 \pm 0.084	806.4 \pm 50.0	0.298 \pm 0.029
4	78.34 \pm 3.68	1.911 \pm 0.090	780.0 \pm 50.7	0.279 \pm 0.029
5	77.46 \pm 3.44	1.889 \pm 0.084	771.7 \pm 48.8	0.273 \pm 0.027
6	79.42 \pm 3.42	1.937 \pm 0.084	791.1 \pm 49.3	0.287 \pm 0.028

Table 4. Accelerometer-based performance summary.

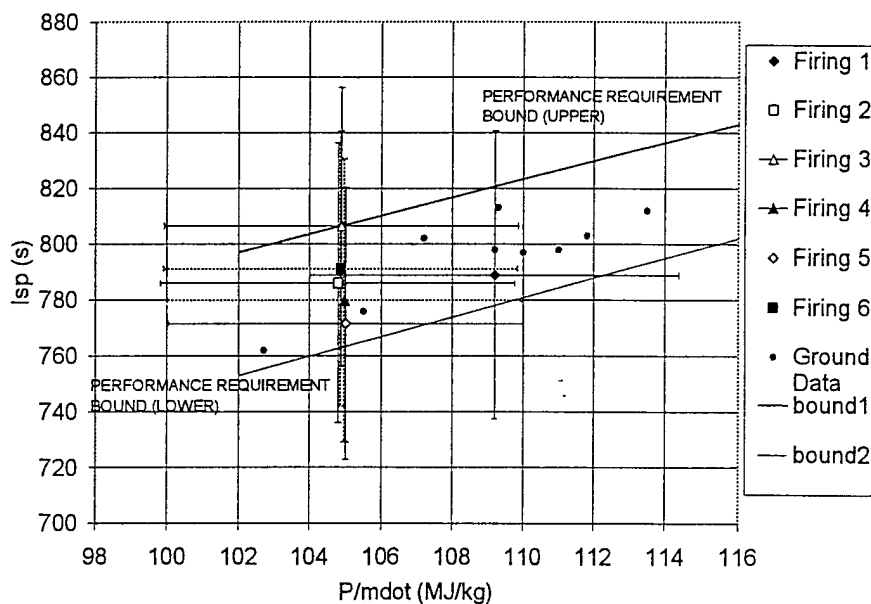


Figure 4. Summary of specific impulse estimates.

Firing	Accelerometer	Radar Ranging	GPS
1	.109 ± .021	.11	.110 ± .003
2	.259 ± .024	.26	N/A
3	.285 ± .028	.27	N/A
4	.401 ± .033	.40	N/A
5	.320 ± .030	.32	N/A
6	.228 ± .022	.23	N/A

Table 5. Total velocity change (m/s) during firings as measured by accelerometer, radar ranging, and GPS.

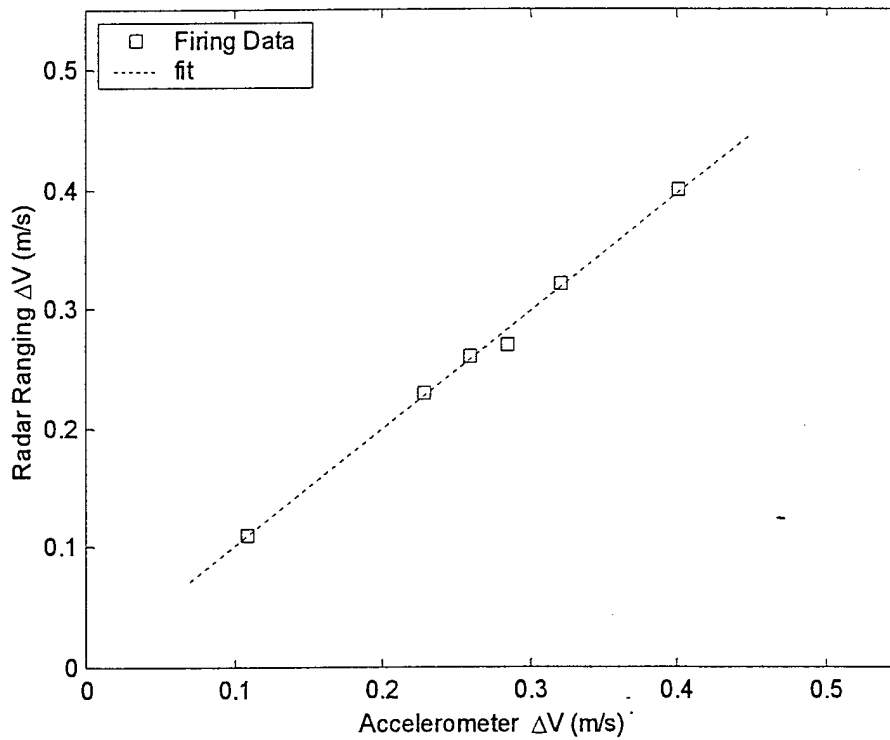


Figure 5. Comparison between ΔV from accelerometer measurement and radar ranging.